Mathematical Model of Technical System in SimScape

Jozef Jenis[1], Jozef Ondriga[1], Patrik Kováčik[1], Matúš Čuchor[1], František Brumerčík[1] and Slavomír Hrček[1]

[1] University of Žilina, Univerzitná 8215/1, 01026 Žilina, Slovakia
jozef.jenis@fstroj.uniza.sk

Abstract. The aim of this paper is to demonstrate the use of MATLAB and Simulink SimScape functions and toolboxes to model and evaluate key properties of an engineering system. In this case, it was a parcel delivery drone. The drone is assembled from four electric motors, propellers, a battery, four structural-bearing arms, and a body that holds the package. The mathematical model of the quadcopter is partitioned based on its subsystems such as sensors, flight dynamics, 3D animation, environment, etc. As science pushes the use of sustainable electronics further and further, the model includes a simplified model of battery performance. The battery capacity for each motor was 7600 mAh, while the 3D printing material had a density of 1400 kg/m^3. The weight of the drone (including batteries and motors) was 2,538 grams carrying a 1 kg package (effective weight ratio). The actuators provided a total maximum thrust of 107 newtons with overall drone dimensions of 48 x 48 x 12 cm. The trajectory was designed to replicate delivery from two locations within a 50 x 50-meter reference plane.

Keywords: Mathematical Modelling, Drone, Trajectory, Matlab, Simulink, SimScape

1 Introduction

Technical system, specifically in this study A quadcopter, also known as a quadrotor, is a helicopter with four rotors. The rotors face up and are arranged in a square formation equidistant from the quadcopter's center of mass. The quadcopter is controlled by adjusting the angular speeds of the rotors, which are turned by electric motors. The quadcopter is a typical design for small unmanned aerial vehicles (UAVs) due to its simple structure. Quadcopters are used for surveillance, search and rescue, construction, package delivery and many other applications [1].

The quadcopter has attracted a lot of attention from researchers because the complex phenomenon of quadcopters has aroused several areas of interest. The basic dynamic model of the quadcopter is the starting point for all studies [2], but more complex aerodynamic properties have also been introduced. Various control schemes were studied, including PID controllers, backstepping controllers, nonlinear controllers, LQR controllers, and nonlinear controllers with nested saturation. Control methods require accurate information from position and attitude measurements made using gyroscopes, accelerometers, and other measurement devices such as GPS, sonar, and laser sensors [3].

M. Petr et al. (eds.), *62nd International Conference of Machine Design Departments (ICMD 2022)*,
Atlantis Highlights in Engineering 28,
https://doi.org/10.2991/978-94-6463-423-5_11

1.1 Conceptual Breakdown of Model

A Mathematical Model was built to simulate the behaviour of an electric-propelled drone. In the **Fig. 1** you can see the 3D model. The model is built from subsystems such as:

1. **Electric Motors** – Necessary to generate torque from battery capacity. Modelled as point masses with a range of 0 – 100 % maximum power capacity. Geometry is imported into MATLAB using STL file format
2. **Propellers** – Used to transform generated torque into useful thrust force that lifts the drone. This is modelled as a linear curve relating the rotation speed and the thrust force
3. **Body of the Drone** – The body of the drone holds all components together and provides rigidity. The design in imported as STL.
4. **Package System** – This constitutes the package [4] that is carried by the drone along with the arms that hold the package in place. As this is regarded as a detail-design feature, the mass was added into the drone body for the mathematical model
5. **Control System** – The control system is necessary to adjust each individual propellor thrust setting such that the drone follows the reference trajectory. In this case a proportional-differential-integral control system is implemented in the model.

Fig. 1. 3D Model of Technical System – Quadcopters.

1.2 Flight Trajectory

The first demonstration of the model is made using a trajectory built from four points: $\boldsymbol{A} = [0, 0, 0]$ $\boldsymbol{B} = [-2, -10, 3]$ $\boldsymbol{C} = [5, -3, 10]$ $\boldsymbol{D} = [7, 2, 10]$

Each coordinate represents the position of the drone in meters relative to the reference point. The total flight distance equates to 40,51 m.

1.3 PID Control System

The drone control system is simplified into a schematic representation in **Fig. 2**. In principle, e(t) is the difference between the current and reference drone position (called

"error"), the u(t) is the reference position and y(t) represent the output position, which feeds back. The controller is a proportional-integral-derivative controller.

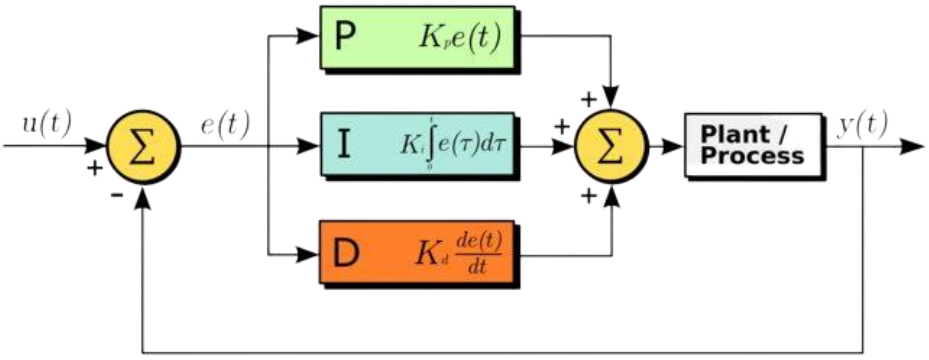

Fig. 2. PID control scheme of drone model.

2 Technical Specifications of the Quadcopters

For a mathematical model to be properly designed [6], the technical system must satisfy certain parameters. These are listed in the following subsections.

- Battery Capacity: 7 600 mAh
- Package Size: 14 x 14 x 14 cm
- Package Mass: 1 kg
- Coefficient of Drag (x / y / z): 0.3 / 0.3 / 0.4
- Density of 3D Material (PLA): 1.4 g/m^3
- Propeller Diameter: 0.155 mm
- Maximum collective thrust: 107 N

2.1 Technical specifications of the Motor

The detailed technical specifications of the motor are presented in **Table 1**. The propellor of choice to base the model on the study undertaken in 2016 in which a solar-powered drone was designed [7]. A recommended power-to- weight ratio for the "Electric glider, Park flyer & Slow Flyer" category is 30 Watts per pound of mass, or 66.22 W/kg. As the drone shall weigh a minimum of 3.5 kg (1 kg package), the minimum power is 231.7 W. **Table 1** presents the technical specifications (diameter is presented in inches) [8].

Table 1. Technical specifications of the Motor [5].

Propeller Diameter	Propeller Pitch	Current (A)	Voltage (V)	Power In (W)	Motor Efficiency (%)	Propeller Thrust (kg)
11	5.5	14.44	10.56	144.58	82.10	0.76

2.2 The Mass Breakdown

The mass breakdown is presented in **Table 2**.

Table 2. The Mass Breakdown.

Component	Mass per unit		Total mass
Propellers	13.5 g		54 g
Electric Drone Motors	34 g		136 g
3D Printed Structure		800 g	
Battery 7600 mAh	387 g		1 548 g
Total mass (excl. package)			**2538 g**

3 Derivation of equations of motion

The flight of the drone can be described using six degrees of freedom, three DOF of position (x, y, z coordinates) and three angles of motion, or so-called Euler angles (bank angle, pitch angle and heading angle). **Fig. 3** depicts the individual angles [9].

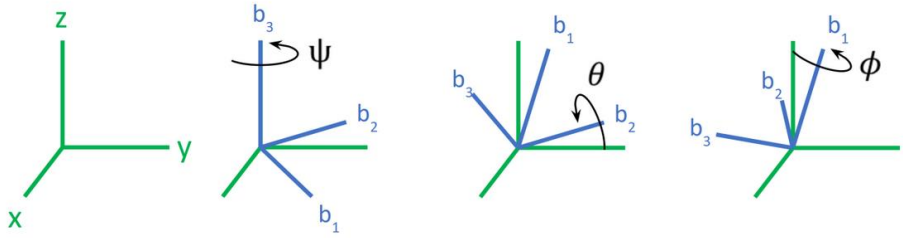

Fig. 3. Angle representation on Quadcopter [9].

Movement of an object is governed by second Newton's law of motion which can be notes as follows:

$$F = \frac{dp}{dt} = m\frac{dv}{dt} = ma \tag{1}$$

$$M = \frac{dH}{dt} = I\frac{d\omega}{dt} = I\Omega \tag{2}$$

The "**I**" represents vector of the moments of inertia and "**Ω**" the vector of angular acceleration. Using the chain rule, the following relations are acquired for a rotating body frame (all with respect to the body frame).

$$F = m(\dot{v} + \omega\ x\ v) \tag{3}$$

$$M = I\omega + \omega\ x\ I\omega \tag{4}$$

Three external forces are considered: Propellor thrust, Gravitational pull, Aerodynamic drag.

3.1 Propeller Thrust

The model does not consider the propellor dynamics, rather assumes the thrust vector to be perpendicular to the propellor and the generated torque about the drone's center of gravity. The thrust vector is as follows:

$$F_z = F_{p1} + F_{p2} + F_{p3} + F_{p4} \tag{5}$$

As for the moment generated it is necessary to determine the positions of the propeller (**Fig. 4**).

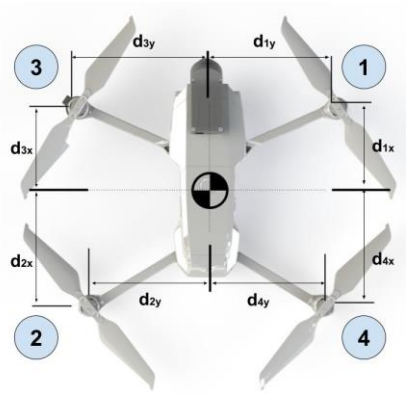

Fig. 4. Position of individual propellors w. r. t. the drone center.

The moments are represented as L, M and L representing pitch, roll and yaw rotations. The yaw rotation is accomplished setting propellors 1 and 2 to rotate counterclockwise, while propellors 3 and 4 rotate clockwise. This setting pushes the air downwards in a way that generates torque about the z-axis and is denoted as a function of N (F, d_x, d_y) [10].

$$L = F_1 * d_{1y} + F_4 * d_{4y} - F_2 * d_{2y} - F_3 * d_{3y} \tag{6}$$

$$M = -F_1 * d_{1x} + F_2 * d_{2x} - F_3 * d_{3x} + F_4 * d_{4x} \tag{7}$$

$$N = -N(F_1, d_{1x}, d_{1y}) - N(F_2, d_{2x}, d_{2y}) + N(F_3, d_{3x}, d_{3y}) + N(F_4, d_{4x}, d_{4y}) \tag{8}$$

3.2 Drag Force

The drag force that acts on the drone structure is dependent on the so-called drag coefficient, the air density, the cross-sectional area (orthogonal to velocity vector) and the velocity of the drone. The equation is as follows:

$$D = C_D * P_{dyn} * S = C_D * \frac{1}{2}\rho v^2 * S \tag{9}$$

The drag coefficient of the drone is simplified for three axes of motion $\left(C_{D_x}, C_{D_y}, C_{D_z}\right)$ CDy, CDz) and three axes of rotation $\left(C_{D_L}, C_{D_M}, C_{D_N}\right)$.

3.3 Thrust Force

The thrust can be considered directly (linearly) proportional to the rotation speed of the propellor in certain design ranges. Diagram **Fig. 5** depicts a comparison of a propellor rig that measured the experimental trust values, which show minuet variation from the linear approximation.

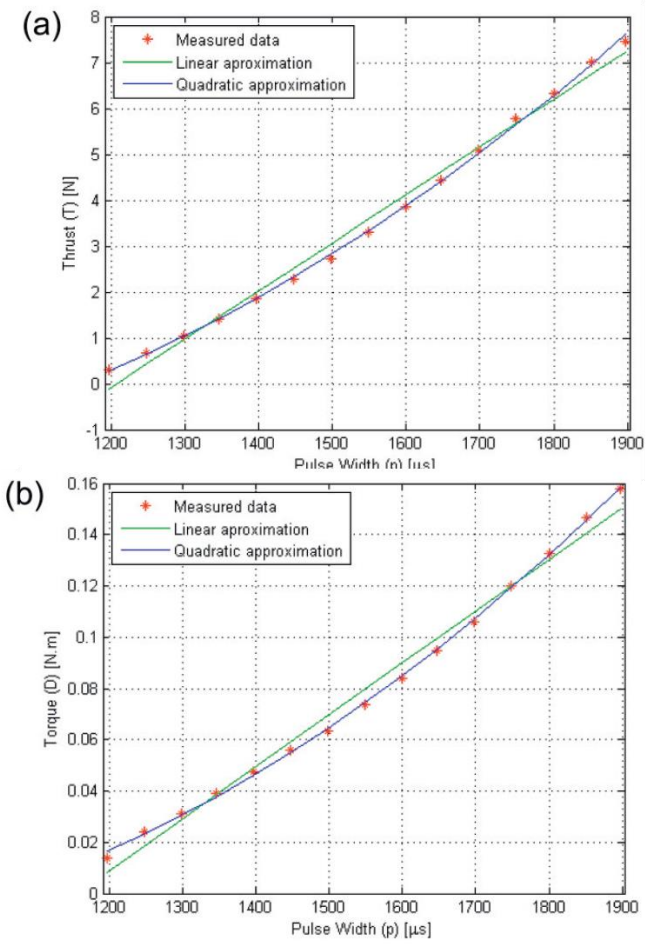

Fig. 5. Linear and quadratic approximation of (a) thrust; (b) torque relative to PWM [11].

4 Matrix-form of differential equations

One of the more popular methods of describing a technical system is known as a state-space system, otherwise also known as the "matrix form". The matrix form describes the set of differential equations and govern [12] the system behavior in a concise fashion. The Quadcopter design is governed by the Newton-Euler method. The inertia vector is defined as:

$$I = \begin{bmatrix} l_{xx} & 0 & 0 \\ 0 & l_{yy} & 0 \\ 0 & 0 & l_{zz} \end{bmatrix} \tag{10}$$

The equations of motion in each direction can be described into the following equation. F denotes the force [13] vector while τ is the torque/moment vector. The second part of the equation denotes the rotating body frame:

$$\begin{bmatrix} mI & 0 \\ 0 & I \end{bmatrix} \begin{bmatrix} a \\ \Omega \end{bmatrix} + \begin{bmatrix} \omega\, x\, (m\omega) \\ \omega\, x\, (I\omega) \end{bmatrix} = \begin{bmatrix} f \\ \tau \end{bmatrix} \tag{11}$$

Simulink solves this system as a linear system according to a specified time step of 0,01 seconds.

5 PID controller of the quadcopter within Simulink

The quadcopter model is so-called “under-actuated”, which describes the fact that the six degrees of freedom are controlled using only four parameters of propellor thrust. Therefore, a minimal amount of two degrees of freedom shall be coupled with the latter. The entire Simulink model is divided into four simple parts, which are very similar to the control feedback principle [14].

5.1 Block 1 - Trajectory definition

The trajectory of x, y and z coordinates must be defined so that the controller is able to measure the reference error [15] term and try to minimize it during flight. For the current model, the trajectory is depicted in Diagram **Fig. 6.** Definition of the drone trajectory.

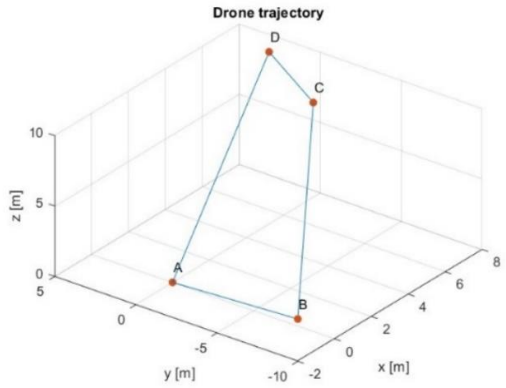

Fig. 6. Definition of the drone trajectory.

The coordinates of the points are as follows:
$\boldsymbol{A} = [0, 0, 0] \quad \boldsymbol{B} = [-2, -10, 3] \quad \boldsymbol{C} = [5, -3, 10] \quad \boldsymbol{D} = [7, 2, 10]$

5.2 Block 2 - Error function

The error function is simply the arithmetic difference between the reference trajectory and the real trajectory of the drone at the given time step.

5.3 Block 3 - Flight Logic

The flight logic (**Table 3**) computer system couples the propellors according to their position. What this means is presented in the table below [16]. Coupling refers to the engagement of the propellors in the same direction and thrust level.

Table 3. Flight logic.

Δe_x	Couple (2 and 4), Couple (1 and 3)
Δe_y	Couple (1 and 2), Couple (3 and 4)
Δe_z	Couple (1,2,3 and 4)

5.4 Block 4 - PID Controller

The PID controller is simplified using the "subsystem" function within which four independent PID controllers are embedded (one PID for each propellor to ensure sufficient sensitivity of external factors) [17].

5.5 Block 5 - Propulsion system

As the "of-the-shelf" drone's design is rather simplistic, the model does not need to consider the angle of the propellor blades [18]. Additionally, the position of the propellor blades is in a fixed position, which greatly simplifies the PID controller. From these simplifications, the model has only four degrees of freedom: the power supplied to the motor from the battery. The Diagram is in **Fig. 7**. Presents the Simulink flow chart from which the input parameter is the current supplied from the battery controller, and the output is the resultant propellor force [19].

$$T = k_T * \rho * n^2 * D^4 \tag{12}$$

$\boldsymbol{k_T}$ – Thrust coefficient (generally in the order of 0,1)
$\boldsymbol{n}$ – Propellor speed (measured in units rev/s)
$\boldsymbol{\rho}$ – Air density at drone height
$\boldsymbol{D}$ – The diameter of the propellor

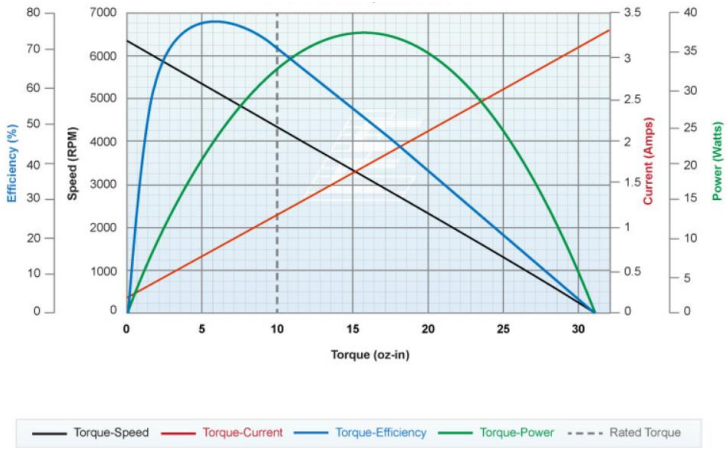

Fig. 7. Technical performance specification of brushless drone motors [20].

5.6 Block 6 - Drone Body and Battery

The propulsion system block is divided into two parts, the motor and the propellor. The motor is modelled based on a brushless induction motor. According to XZ (AAA), the torque generated by the motor type is linear w.r.t to the electric current passing through it. The technical characteristics of the model BL16B17-08 is depicted in **Fig. 8** [20].

The drone body included the mass of all the components alongside the package weight, including the moments [21] of inertia about all three axes. As the model is assumed symmetric, all cross-moments of inertia are zero. The current used by the motors is simply subtracted every second from the battery capacity (no thermal or electrostatic influences). The external forces (gravitational pull) are also within this block [22].

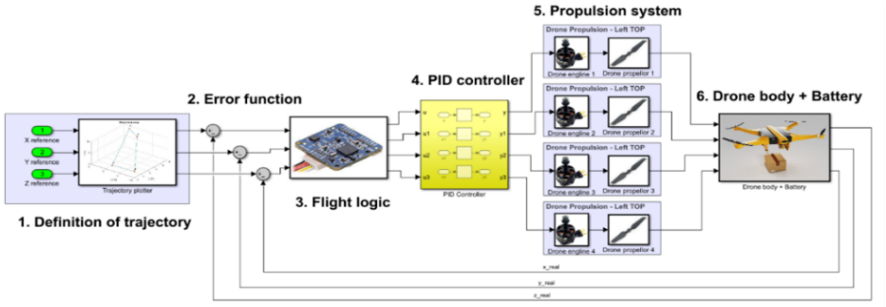

Fig. 8. Full architecture of the Quadcopter using SimScape.

6 Results and Discussion

The results showed a maximum vertical velocity of 0,515 m/s. The flight time was 148 seconds for two-way flight with 4 distinct points (total flight trajectory length of 40,51

m). For the given flight, an average velocity of 0,21 m/s was achieved. A total capacity of 2 800 mAh was spent (9 % charge), which is significantly higher than in comparison with real flight data from literature research. Diagram **Fig. 9** depicts the state of discharge along with the maximum current readings for each propellor.

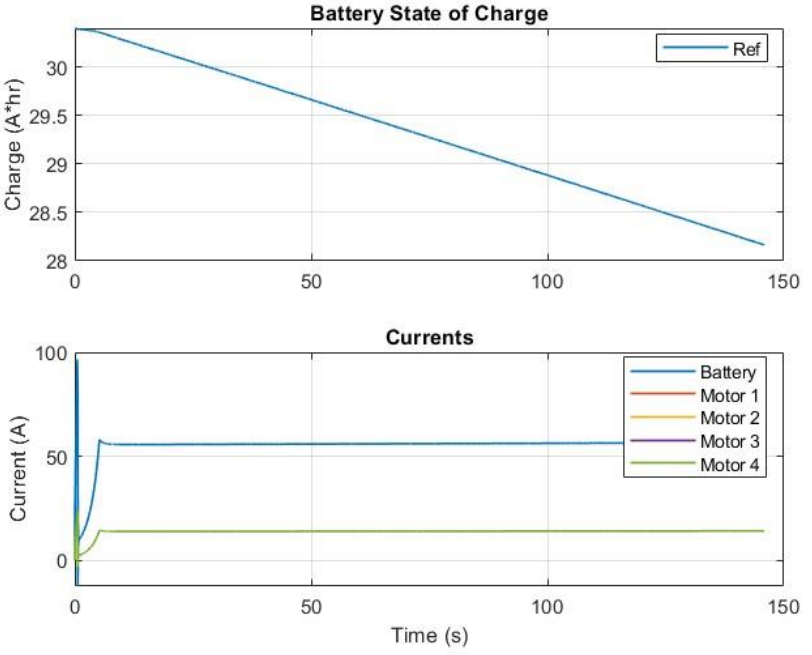

Fig. 9. Battery use during flight.

Further research of the model shall dive into the challenge of optimizing the key drone parameters. The geometry, control and motors shall be optimized with the use of both classic methods (such as gradient descent, particle swarm optimalization) and neural networks / machine learning algorithms (such as method of nearest neighbor or convoluted neural networks).

Such research can be applied to any technical system. This means that a technical model is first built and then its architecture can be used to investigate various parameters and results by means of simulations and various calculations. Something similar has already been applied to high-precision harmonic transmissions, where the mathematical model of the harmonic transmission was used to detect just the global sensitivity analysis of the various design parameters affecting the lossy motion of the harmonic transmission. The research was done on two harmonic drives with the same ratio but different dimensions and power ratings to generalize and correctly interpret the analysis results. The most important variable of the tested set of parameters affecting the value of the lost motion for both harmonic drive units was the displacement from the nominal tooth shape affecting the dimensions above the flex groove pin and the dimension between the circular groove pin [23].

7 Conclusion

The mathematical modeling and control of a quadcopter were investigated in this article. The mathematical model of quadcopter dynamics was described, and differential equations derived from the Newton-Euler and Euler-Lagrange equations were presented. The model was validated by simulating quadcopter flying with Matlab and Simulink (SimScape). The quadcopter's attitude was stabilized by using a PID controller. To control the quadcopter's trajectory, a heuristic technique was created. The PD controller was implemented into the heuristic technique to improve reaction to disturbances in the quadcopter's flight circumstances.

Only simulations were used to test the provided model and control approaches. To acquire more realistic and dependable findings, an actual experimental quadcopter prototype should be built. Even if building an actual quadcopter and estimating all model parameters are time-consuming processes, a genuine quadcopter would significantly improve the research. The theoretical framework and simulation findings might be compared to real-life measurements using an actual prototype. This research did not contain these highlighted issues, but instead presented the fundamentals of quadcopter modeling and control. This article can potentially be used as a springboard for future research into more advanced quadcopter modeling.

Acknowledgments. This publication was realized with the support of Operational Program Integrated Infrastructure 2014 - 2020 of the project: Research and development of the usability of autonomous aircraft in the fight against the pandemic caused by COVID-19, code ITMS 313011ATR9, co-financed by the European Regional Development Fund.

Acknowledgments. This study was supported by the Slovak Research and Development Agency under contract no. APVV-18-0450 - Research of the influence of design parameters of special transmissions with a high gear ratio with respect to kinematic properties.

References

1. Luukkonen, T. (2011). Modelling and control of quadcopter. Independent research project in applied mathematics, Espoo, 22, 22.
2. Abdelhay, S., & Zakriti, A. (2019). Modeling of a quadcopter trajectory tracking system using PID controller. Procedia Manufacturing, 32, 564-571.
3. Čačo, M., Kohár, R., Hrček, S., Tribula, R., & Ščerba, P. (2017). Use the method of TRIZ in optimizing automated machine for ultrasonic welding. Procedia engineering, 192, 80-85.
4. Kučera, Ľ., Patin, B., Gajdošík, T., Palenčár, R., Palenčár, J., & Ujlaky, M. (2020). Application of metrological approaches in the design of calibration equipment for verification of float level gauges. Measurement Science Review, 20(5), 230-235.

5. Benić, Z., Piljek, P., & Kotarski, D. (2016). Mathematical modelling of unmanned aerial vehicles with four rotors. Interdisciplinary Description of Complex Systems: INDECS, 14(1), 88-100.
6. Orman, L., Radek, N., & Bronček, J. (2018). Sintered mesh layers for the production of efficient phase–change heat exchangers. Materials Research Proceedings.
7. Majchrák, M., Kohár, R., Kajan, J., & Skyba, R. (2019). 3d meshing methods of ball-rolling bearings. Transportation Research Procedia, 40, 784-791.
8. Rajendran, P., Smith, H., Yahaya, K. I., & Mazlan, N. M. (2016). Electric propulsion system sizing for small solar-powered electric unmanned aerial vehicle. International Journal of Applied Engineering Research, 11(18), 9419-9423.
9. Tytler, C. (2017). Modeling Vehicle Dynamics–Quadcopter Equations of Motion. URL: https://charlestytler. com/quadcopterequations-motion/. Online.
10. Weis, P., Kučera, Ľ., Pecháč, P., & Močilan, M. (2017). Modal analysis of gearbox housing with applied load. Procedia engineering, 192, 953-958.
11. Chovancová, A., Fico, T., Chovanec, Ľ., & Hubinsk, P. (2014). Mathematical modelling and parameter identification of quadrotor (a survey). Procedia Engineering, 96, 172-181.
12. Jambor, M., Kajanek, D., Fintová, S., Bronček, J., Hadzima, B., Guagliano, M., & Bagherifard, S. (2021). Directing Surface Functions by Inducing Ordered and Irregular Morphologies at Single and Two-Tiered Length Scales. Advanced Engineering Materials, 23(2), 2001057.
13. Majchrák, M., Kohár, R., Lukáč, M., & Skyba, R. (2020). Creation of a computational 2d model of harmonic gearbox. In Current Methods of Construction Design (pp. 95-103). Springer, Cham.
14. Kucera, L., Gajdac, I., & Kamas, P. (2014). Computing and design of electric vehicles. In Modern Methods of Construction Design (pp. 105-111). Springer, Cham.
15. Wang, P., Man, Z., Cao, Z., Zheng, J., & Zhao, Y. (2016, November). Dynamics modelling and linear control of quadcopter. In 2016 International Conference on Advanced Mechatronic Systems (ICAMechS) (pp. 498-503). IEEE.
16. Khan, M. (2014). Quadcopter flight dynamics. International journal of scientific & technology research, 3(8), 130-135.
17. Gramblička, S., Kohár, R., & Madaj, R. (2017). Construction design automatically adjustable mechanism for crane forks. In ICMD 2017, Proceedings of the 58th international conference of machine design departments. Czech University of Life Sciences Prague (pp. 100-103).
18. Ostojić, G., Stankovski, S., Tejić, B., Đukić, N., & Tegeltija, S. (2015). Design, control and application of quadcopter. International Journal of Industrial Engineering and Management, 6(1), 43.
19. https://web.mit.edu/16.unified/www/FALL/thermodynamics/notes/node86.html, last accessed 2022/09/28.
20. https://uav.jreyn.net/quadcopter-design/step-5-motor-selection, last accessed 2022/09/28.
21. Kučera, Ľ., & Gajdošík, T. (2014). The vibrodiagnostics of gears. In Modern Methods of Construction Design (pp. 113-118). Springer, Cham.
22. ČAČO, M., TRIBULA, R., ŠČERBA, P., & KOHÁR, R. (2017). Application of simulation software to optimize construction nodes of ultrasonic welding machines.
23. Hrcek, S., Brumercik, F., Smetanka, L., Lukac, M., Patin, B., & Glowacz, A. (2021). Global Sensitivity Analysis of Chosen Harmonic Drive Parameters Affecting Its Lost Motion. Materials, 14(17), 5057.